

Half-cell Study of La and Ca doped Strontium Titanates Anode for Direct Methane Solid Oxide Fuel Cell

Pankaj Kr. Tiwari^a, John TS Irvine^b, Suddhasatwa Basu^{a*}

^aDepartment of Chemical Engineering, Indian Institute of Technology Delhi
New Delhi 110016, India

^bSchool of Chemistry, University of St. Andrews, Fife KY 16 9ST, Scotland,
UK

*Corresponding Author Email: sbasu@iitd.ac.in; Tel. +91-11-26591035

Abstract

Solid oxide fuel cell (SOFC) has been providing high conversion efficiency of chemical energy to electricity without any pollution. One of the major advantages of SOFC over other fuel cell is use of direct natural gas at high temperature without any external reformer. Conventional nickel-yttria stabilized zirconia (Ni-YSZ) composite anode provides excellent catalytic property, current collection and stability for H₂ oxidation but it is not tolerant towards sulphur poisoning and also accelerates coke deposition in presence of hydrocarbon fuels. It necessitates the use of alternate anode for direct hydrocarbon fuel. In the present work, attempts have been made to apply La and Ca doped A-site deficient SrTiO₃ (LSCT_{A-}) as potential anode for direct methane SOFC. Low catalytic activity of LSCT_{A-} is improved by infiltration of Ni and CeO₂ catalyst. Half cell (YSZ/4%Ni-6%CeO₂-LSCT_{A-}) provided 200 mW cm⁻² maximum power density and regain its initial performance in H₂ even after 6 h exposure to humidified CH₄ at 800 °C.

Introduction

Solid oxide fuel cell (SOFC) is a promising power device in scenario of current global environmental issues and increased demand for alternative energy sources. SOFC is highly efficient and require no external reformer as it directly converts hydrocarbon fuel to electrical energy. Oxidation of fuel takes place at anode so choice of high catalytic active and efficient anode material is the most important consideration in direct hydrocarbon SOFC. Conventionally, nickel (Ni) is widely used as anode because of its excellent catalytic property, current collection and stability towards H₂ oxidation but it is not tolerant to sulphur poisoning and also accelerates coke deposition in presence of hydrocarbon fuels. Coke deposition drastically degrades the SOFC performance. Significant reduction in the coke deposition using anodes such as Cu-CeO₂ and Fe-CeO₂ has been observed (1-3). Thermal instability and limited electrochemical activity of copper based anodes at SOFC operation temperature need use of alternate anode materials for sustained stable performance in presence of direct hydrocarbon fuels (4-5). Agglomeration of Ni particles due to sintering leads to cell deactivation during operation at high temperature (800 °C), which is another major

concern. Transition Metal oxides such as TiO_2 , CeO_2 and Nb_2O_5 in small amount (~5-10 wt %) are added to Ni-YSZ anode to prevent performance degradation due to Ni coarsening (6-9). Recently, single and double doped SrTiO_3 (both at A and B site) has been researched extensively and it exhibited that doped SrTiO_3 not only prevent the loss due Ni sintering but also provides a excellent alternate to Ni based anode for hydrocarbon fuels. Higher valent cation such as La^{3+} when substituted at Sr^{2+} site induce semiconducting behavior in SrTiO_3 . The substitution of Sr^{2+} with La^{3+} can be compensated by introducing the extra oxygen beyond the ABO_3 stoichiometry under oxidizing conditions and maintains the electro-neutrality. Strontium titanate (SrTiO_3) possesses desirable thermal and chemical stability and show mixed ionic and electronic conducting (MIEC) behavior at low oxygen partial pressure (10-12). It is shown that A-site deficiency enhances the electrical conductivity of La^{3+} doped SrTiO_3 (13-15). Ca doping lowers down the sintering temperature of LST_A - backbone and enhances the reducibility and electrical conductivity (13). Catalytic activity of LSCT_A - towards fuel oxidation has been improved by infiltration of transition metal and metal oxides such as Cu, Ni and CeO_2 (13, 16-17).

In the current work, A-site deficient $\text{La}_{0.2}\text{Sr}_{0.25}\text{Ca}_{0.45}\text{TiO}_3$ (LSCT_A -) anode backbone is fabricated, characterized and used in electrolyte supported half-cells. LSCT_A -backbone is impregnated with nitrate precursors of Ni and/or CeO_2 to increase the catalytic activity and the cell performances in H_2 and humidified CH_4 at 800 °C (18-19). The present work explores the potential of La and Ca co-doped A-site deficient SrTiO_3 anode for direct methane SOFC.

Experimental

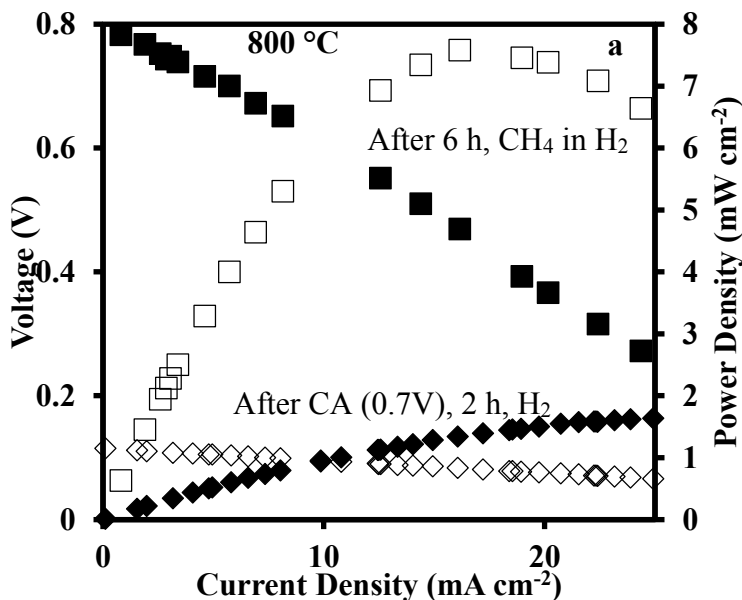
Aqueous tape casting and co-sintering of dense YSZ electrolyte and porous $\text{La}_{0.2}\text{Sr}_{0.25}\text{Ca}_{0.45}\text{TiO}_3$ (LSCT_A -) anode has been carried out to fabricate half-cells (18-19). The LSCT_A - powder for anode was mixed with graphite (pore former) and milled for 24 h by adding de-ionized water as solvent, hypermer KD 6 as dispersant. Poly(ethylene glycol), glycerol as plasticizer, poly vinyl alcohol and ethoxylated 2,4,7,9-tetra ethyl 5 decyn-4,7-diol as deformer were added to the slurry and milled for next 24 h. After that, suspension was de-aired and cast to get green tapes. Similarly, dense YSZ green tapes were casted. Green tapes of LSCT_A - and YSZ were laminated together to get dense YSZ/porous LSCT_A -. Then green laminated tapes were cut in to appropriate size and co-sintered at 1350 °C. The sintered anode was reduced in H_2 atmosphere at 950 °C. CeO_2 and/or Ni catalyst were impregnated in LSCT_A - porous anode matrix using $\text{Ce}(\text{NO}_3)_3 \cdot 6\text{H}_2\text{O}$ and $\text{Ni}(\text{NO}_3)_2 \cdot 6\text{H}_2\text{O}$ solution (18-19). Multiple impregnation and calcination at 500 °C were carried out till required loading in porous LSCT_A - was achieved. Silver wire current collectors were applied to both the electrodes using silver paste and active area of cell was 0.5 cm^2 . Cell was sealed onto ceramic tube using Aremco, Ceramabond 552. Hydrogen (H_2) or humidified methane (CH_4) gas was supplied with flow rate of 50 mL/min to the anode. The current-voltage characteristics followed by impedance studies at open circuit voltage (OCV) were carried out using potentiostat/galvanostat (Autolab, Metrohm). The microstructure, morphology and elemental mapping of half-cells before and after cell operation had been analyzed using scanning electron microscope (SEM) and energy dispersive x-ray spectroscopy (EDX) using Zeiss EVO 50. The

particle size and selected area diffraction patterns were observed using HR-TEM (TEM, Technai G² 200 KV, FEI).

Result and Discussion

Electrolyte supported half-cell testing

Electrolyte (YSZ) supported half-cell with LSCT_A- as anode has been electrochemically characterized in H₂ and humidified CH₄ fuel at 800 °C to assess the electro catalytic activity of LSCT_A- (fig. 1a-b). Cell is operated in H₂ fuel at 800 °C for 2 h and very low open circuit voltage (OCV) is observed. To activate the anode, chronoamperometry (CA) at 0.7 V has been carried out for 45 minute and OCV increases up to 0.1 V, which is still very low. After 3 h in H₂, humidified CH₄ is supplied as fuel to anode chamber. The OCV of cell slowly increases and after 6 h exposure to CH₄ in presence of H₂ fuel, 0.8 V OCV is recorded. LSCT_A- anode shows poor catalytic activity towards H₂ and CH₄ oxidation as cell performance in terms of current and power density is very low as presented in fig. 1a. At 1 h of cell operation in H₂, 0.86 ohm cm² ohmic resistance is observed which increases to 4.89 ohm cm² at 6 h of cell operation in humidified CH₄ but decreases down to 1.735 ohm cm² in presence of H₂ fuel after 6 h exposure of CH₄. The polarisation resistance increases from 0.212 at 1 h in H₂ to 2.60 ohm cm² at 6 h operation in CH₄. Inset of fig. 1b shows the impedance spectra corresponds to 1 h operation in H₂ and after CA (0.7V) at 2 h of operation. It can be infer from above mentioned analyses that LSCT_A- is catalytically inactive for methane decomposition but it does not get deteriorated due to the coke deposition during operation as evident from the decrement in resistance and enhanced OCV in H₂ atmosphere after CH₄ exposure for 6 h. Carbon particles provides the conducting pathway instead of blocking the active surface hence better result in H₂ after CH₄ exposure. To increase the catalytic activity of anode backbone, impregnation of the porous LSCT_A- with active metal catalyst has been carried out and corresponding results are presented here.



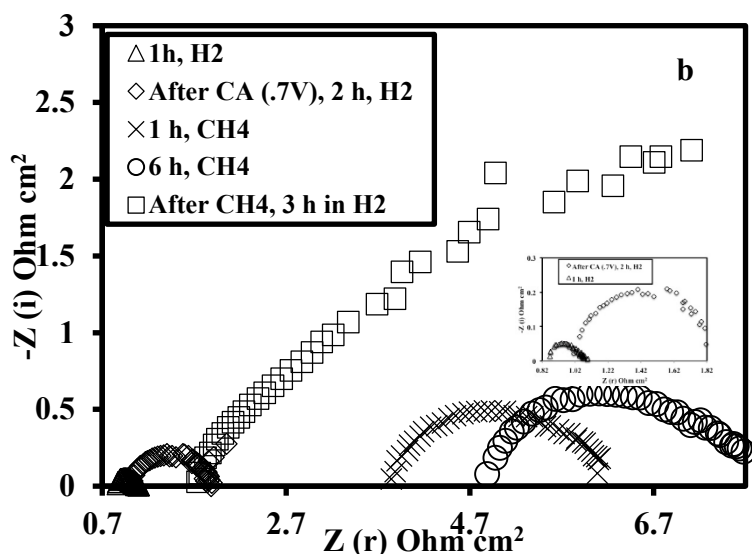


Fig. 1 (a) i-V characteristics, (b) Impedance spectra at OCV of half cell (YSZ/LSCT_A-) in H₂ and humidified CH₄ at 800 °C.

Fig. 2(a-b) shows SEM of fracture surface and LSCT_A- anode after cell testing. The thickness of electrolyte and anode are 300 and 100 μm respectively. Electrolyte is perfectly dense and proper adherence between electrolyte and anode is observed even after 12 h of cell operation at 800 °C. Fig 2b shows well connected grains of LSCT_A- with sufficient porosity in stable anode backbone structure. Average particle size is ~ 1-2 μm. After cell testing HRTEM of LSCT_A- is carried out. Fig. 3 shows HRTEM of agglomerated LSCT_A- particles. Diffraction patterns correspond to crystalline nature of LSCT_A- is shown in the fig. 3a. SAED pattern in fig 3b shows regular crystal diffraction pattern corresponds to LSCT_A- crystal.

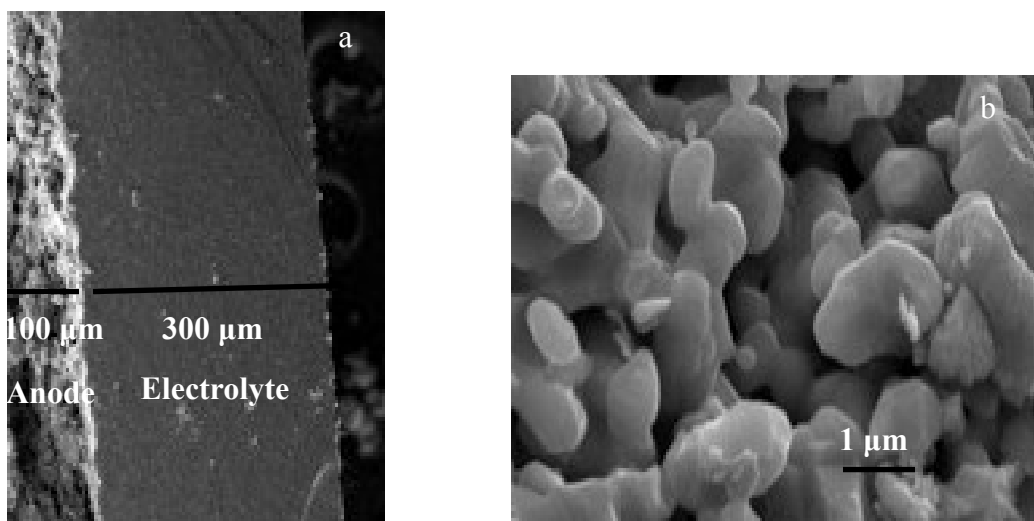


Fig. 2 (a) SEM of (a) Fracture surface and (b) Anode of half cell (YSZ/LSCT_A-) after testing in H₂ and humidified CH₄.

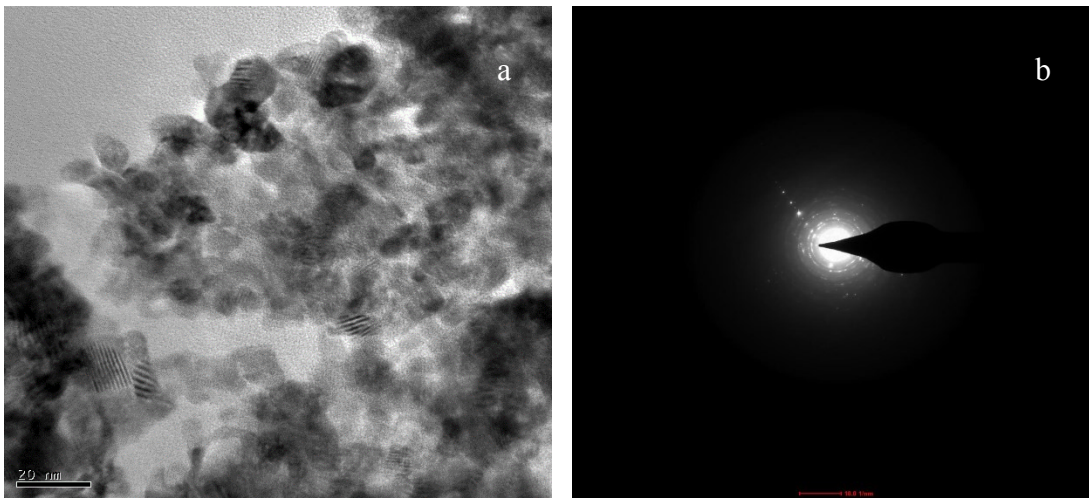


Fig. 3 (a) HRTEM and (b) SAED of LSCT_A- after testing in H₂ and humidified CH₄.

To enhance the catalytic activity, 6% CeO₂ is impregnated in porous LSCT_A- anode and tested in electrolyte supported half-cell in H₂ and humidified CH₄ at 800 °C. Fig. 4(a-b) presents the i-V, i-P and impedance spectra of YSZ/6%CeO₂-LSCT_A- half cell. As shown in fig. 4a, maximum power density 132 mW cm⁻² (305 mA cm⁻²) is observed at 1 h in H₂ fuel. After 3 h of cell operation in H₂, humidified CH₄ is fed as fuel. Maximum power density in CH₄ after 6 h is 70 mW cm⁻² (174 mA cm⁻²), which is lower than that of the power density observed in H₂. The half cell regains its initial performance once the H₂ is again fed and maximum power density 111 mW cm⁻² (305 mA cm⁻²) has been observed. The performance degradation in CH₄ is due to sluggish reaction associated with the dissociation of CH₄. It is significant to note that degradation in performance due to CH₄ is not drastic and reasonable performance is shown by cell even after 6 h exposure of CH₄ during operation at 800 °C. It has been observed from impedance analyses, shown in fig. 4b that ohmic as well as polarisation resistance in H₂ is not changed significantly before and after 6 h operation in humidified CH₄. Ohmic and total polarization in H₂ and CH₄ changed from 0.832 to 1.531 ohm cm² and 0.38 to 0.7574 ohm cm² respectively. In CH₄, the ohmic as well as polarization resistance increased significantly which might be due to sluggish reaction kinetics corresponds to CH₄ oxidation on LSCT_A- backbone. Presence of CeO₂ enhances the ionic conductivity as well as catalytic activity in anode backbone and does not accelerate the coke formation as infer from the above discussion. Morphological and elemental analysis of cell after 12 h of operation is presented in fig. 5(a-c). Well-distributed fine nano sized CeO₂ particles on LSCT_A- backbone as well as in the pores can be seen from fig. 5a. HRTEM in fig. 5b shows the diffraction patterns correspond to LSCT_A- crystal. SAED pattern shown in inset of fig. 5c confirms the crystalline CeO₂ along with the regular pattern corresponds to LSCT_A-. Presence of constituent elements La, Sr, Ca, Ti, O and Ce in anode is confirmed from the EDX analysis after operation as presented in fig. 5c.

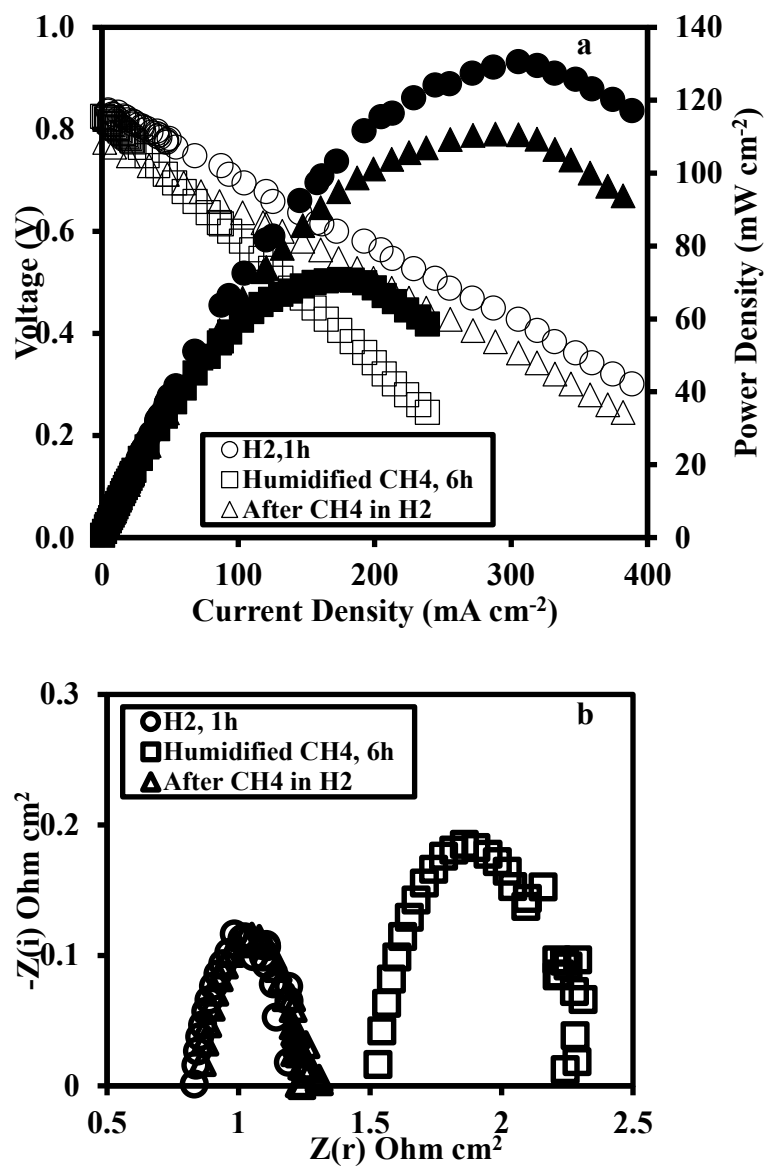
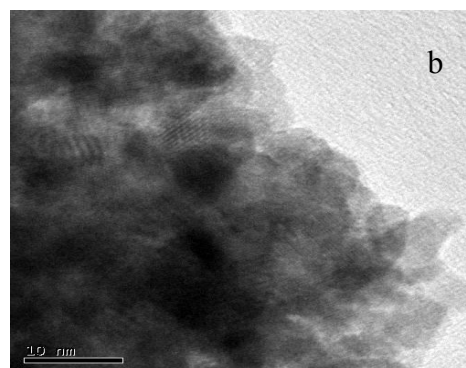
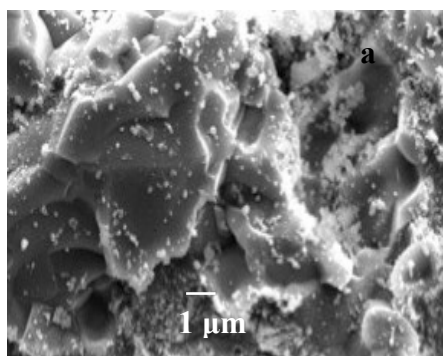


Fig. 4 (a) i-V characteristics, (b) Impedance spectra at OCV of half cell (YSZ/6%CeO₂-LSCT_A) in H₂ and humidified CH₄, 800 °C.



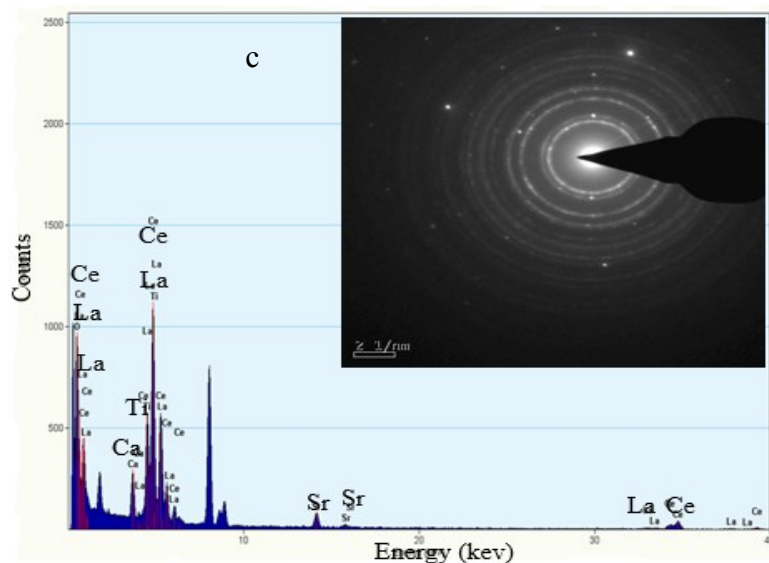


Fig. 5 (a) SEM, (b) HRTEM and, (c) Elemental analysis, SAED of anode of half cell (YSZ/6%CeO₂-LSCT_A) after testing in H₂ and humidified CH₄.

4% Ni is impregnated along with the 6% CeO₂ in porous LSCT_A anode to enhance the half-cell performance by increasing catalytic activity. i-V, i-P and impedance analysis of half-cell shown in fig. 6 (a-b) explains the performance in H₂ as well as in CH₄ at 800 °C. Maximum power density of cell is 200 mW cm⁻² (554 mA cm⁻²) at 1 h of operation in H₂, which increases up to 216 mW cm⁻² (578 mA cm⁻²) in H₂ after 6h of cell operation in humidied CH₄. In humidified CH₄ exposure, maximum power density of cell is 89 mW cm⁻² (285 mA cm⁻²) at 1 h of operation, which increases up to 140 mW cm⁻² (409 mA cm⁻²) at 6 h of operation. At elevated temperature the LSCT_A backbone along with the catalysts is getting reduced further hence the increase in performance with time has been observed. Improved performance also indicates that Ni particles in presence of CeO₂ are not get agglomerated due to sintering at elevated temperature. This phenomenon suggests strong metal support interaction (SMSI) between Ni and CeO₂. Similar behavior between Ni and TiO₂ on YSZ backbone has been reported earlier (6-7). Lower performance in CH₄ is due to the sluggish reaction corresponding to CH₄ oxidation. So, it can be infer here that Ni is not promoting the coke deposition in presence of CeO₂, as reasonable performance is observed in humidified CH₄ environment and even in H₂ atmosphere after CH₄ exposure for 6 h at 800 °C. i-V and i-P analyses are corroborated with the impedance results presented in fig. 6 b. It is observed that the ohmic as well polarization resistance decreases in H₂ before and after CH₄ exposure. Ohmic resistance decreases from 2.083 to 1.376 ohm cm² before and after 6 h operation in CH₄ respectively. The decrease in ohmic resistance may be due to deposition of carbon particles in anode matrix during operation in CH₄.

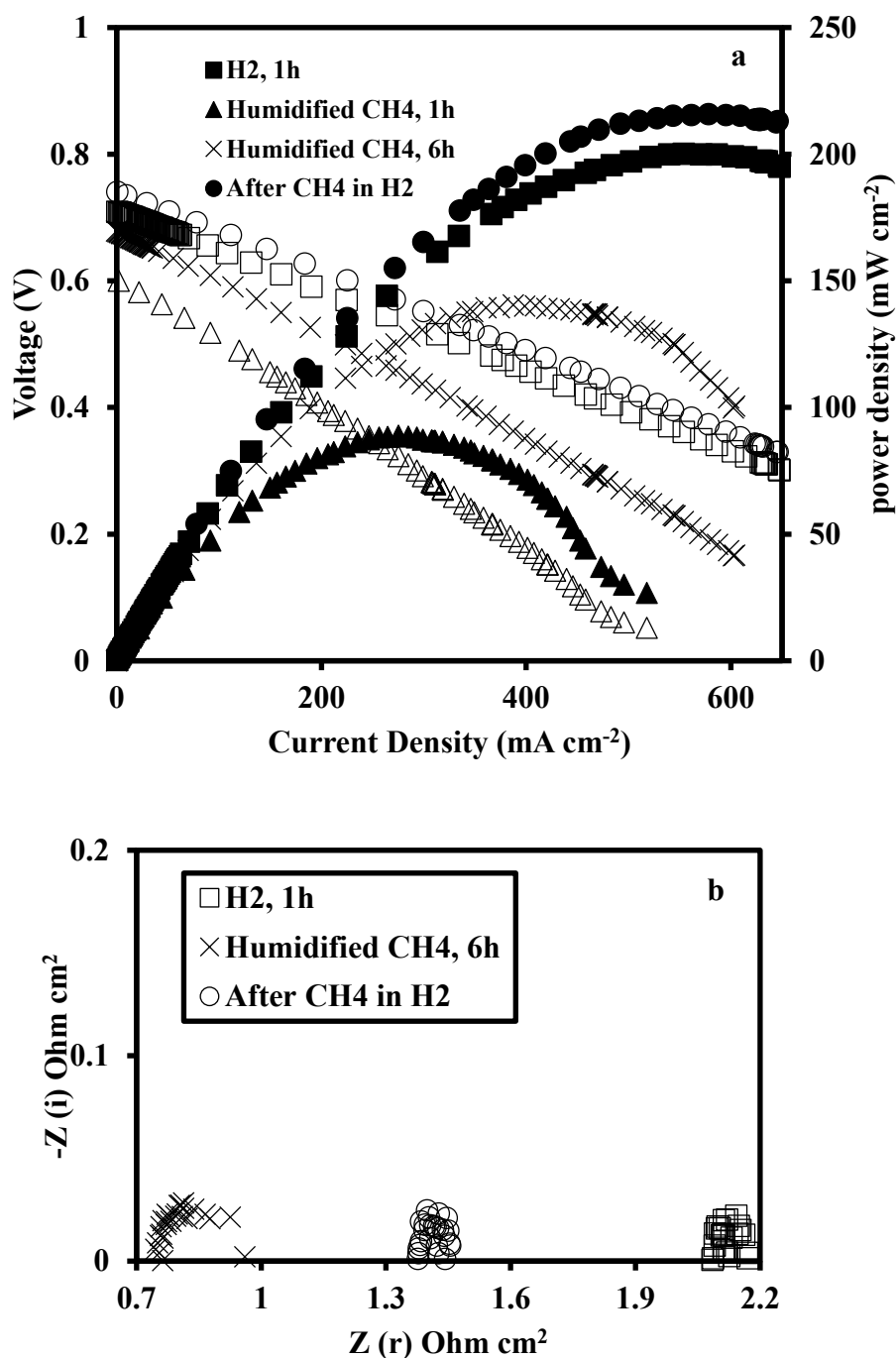


Fig. 6 (a) i-V characteristics, (b) Impedance spectra at OCV of half cell (YSZ/4% Ni-6% CeO₂-LSCT_{A-}) in H₂ and humidified CH₄, 800 °C.

Recently published work by researchers from Irvine group (19) reported enhanced performance of LSCT_{A-} in presence of small amount of Ni and CeO₂ in H₂ atmosphere but they did not explore the viability of LSCT_{A-} in CH₄. Fig. 7 (a-b) represents the morphology, HRTEM and SAED pattern of cell after operation for 12 h. SEM micrograph (fig.7a) shows the well-dispersed Ni/CeO₂ anode catalyst on and in the pores of LSCT_{A-}. Well-patterned grains of LSCT_{A-} as well as finely dispersed Ni/CeO₂ particles on and around LSCT_{A-} can be observed from fig.7b. It has been

observed that other than regular crystal diffraction patterns some separate patterns correspond to Ni/CeO₂ are also present in SAED as shown in the inset of fig. 7b.

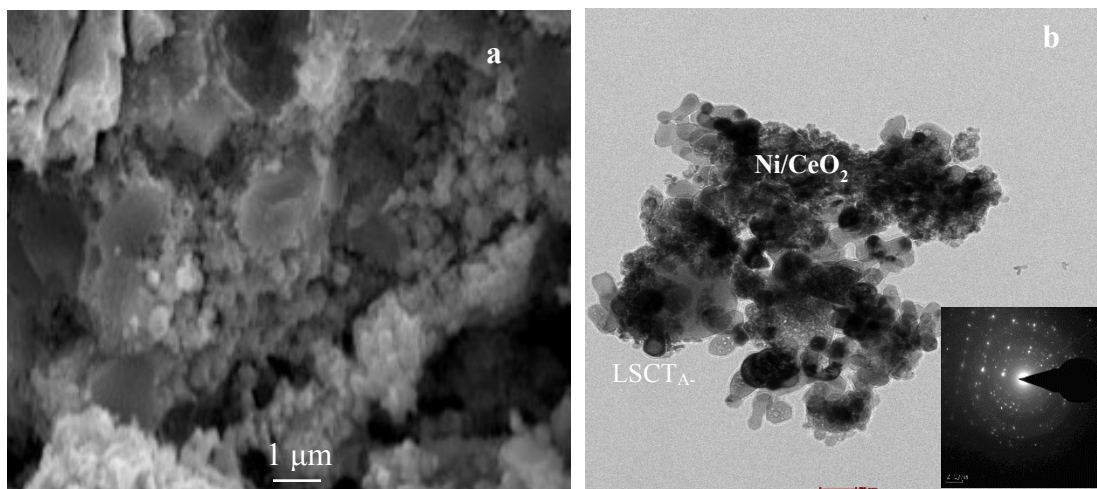


Fig. 7 (a) SEM, (b) HRTEM and SAED of anode of half cell (YSZ/4%Ni-6%CeO₂-LSCT_A-) after testing in H₂ and humidified CH₄, 800 °C

Conclusion

Electrolyte supported half-cells with LSCT_A- anode backbone have been tested in H₂ and humidified CH₄ fuel. Low catalytic activity of LSCT_A- towards electro oxidation of fuel is significantly improves in presence of metallic catalyst. 6% CeO₂ loading in LSCT_A- backbone improves the performance of the cell in H₂ as well as in humidified CH₄ at 800 °C. It has been observed that coke deposition did not degrade the anode active surface even after 6 h of exposure of CH₄ at elevated temperature. 4% Ni infiltration in 6% CeO₂-LSCT_A- enhances the performance from 131 mW cm⁻² to 200 mW cm⁻² at 800 °C in H₂. In humidified CH₄ environment, cell having 4% Ni-6% CeO₂-LSCT_A- anode shows low performance (140 mW cm⁻² Power density) due to sluggish methane oxidation reaction but provided enhanced power density (216 mW cm⁻²) once H₂ is again fed after 6 h cell operation in humidified CH₄. Performance of the cell is reasonably good as results presented here correspond to cells having thick electrolyte (300 μm). Cells are structurally robust even after 12 h of accelerated testing. LSCT_A- is a potential anode backbone material for direct methane SOFC and could be an excellent anode for other hydrocarbons.

References

1. R. J. Gorte and J. M. Vohs, *J. Catalysis*, **216**, 477 (2003).
2. S. K. Lee, A. Kipyung, J. M. Vohs and R. J. Gorte, *Electrochem. Solid-State Lett.*, **8**, A48 (2005).
3. G. Kaur and S. Basu, *J. Power Sources*, **241**, 783 (2013).
4. G. Kaur and S. Basu, *Fuel Cells*, **14**(6), 1006 (2014).

5. G. Kaur and S. Basu, *Int. J. Energy Res.*, **39**, 1345 (2015).
6. C. A. Singh, L. Bansal, P. Tiwari and V. V. Krishnan, *ECS Trans.*, **25**(2), 897 (2009).
7. P. Tiwari and S. Basu, *Int. J. Hydrogen Energy*, **38**, 9494 (2013).
8. P. Tiwari and S. Basu, *J. Solid State Electrochem.*, **18**, 805 (2014).
9. P. Tiwari and S. Basu, *ECS Trans.*, **57**(1), 1545 (2013).
10. C. Sun and U. Stimming, *J. Power Sources*, **171**, 247 (2007).
11. S. Tao and J. T. S. Irvine, *J. Mater. Chem.*, **12**, 2356 (2002).
12. S.W.Tao and J.T.S.Irvine, *Chemical Record*, **4**(2), 83 (2004).
13. A. D. Aljaberi and J.T.S. Irvine, *J. Mater. Chem. A*, **1**, 5868 (2013).
14. C. D. Savaniu and J.T.S. Irvine, *Solid State Ionics*, **192**, 491 (2011).
15. P. Tiwari and S. Basu, *ECS Trans.*, **68** (1), 1435 (2015).
16. A. Yaqub, C. D. Savaniu, N. K. Janjua and J. T. S Irvine, *J. Mater. Chem. A*, **1**, 14189 (2013).
17. M. C. Verbraeken, B. Iwanschitz, A. Mai and J. T. S. Irvine, *J. Electrochem. Soc.*, **159** (11), F757 (2012).
18. L. Lu, M. C. Verbraeken, M. Cassidy and J. T. S. Irvine, *ECS Trans.*, **57**(1), 1415 (2013).
19. L. Lu, C. Ni, M. Cassidy and J.T.S. Irvine, *J. Mater. Chem.*, **4**, 11708 (2016).